Nanomed Res J 8(1):37-49, Winter 2023

RESEARCH ARTICLE

DSPC based polymeric micelles loaded with Amphotericin B: synthesis, characterization, and in vitro study

Khadijeh Rajablou[1]; Hossein Attar[1,*]; Seyed Kazem Sadjady[2]; Amir Heydarinasab[1]

[1] Department of Petroleum and Chemical Engineering, Science and Research Branch, Islamic Azad University, Tehran, Iran
[2] Department of Pharmaceutics, Faculty of Pharmacy, Tehran Medical Sciences, Islamic Azad University (IAU), Tehran, Iran

ARTICLE INFO

Article History:
Received 24 Feb 2023
Accepted 06 Mar 2023
Published 08 Mar 2023

Keywords:
Amphotericin B
DSPC
Polymeric micelles
Drug encapsulation
Antifungal activity

ABSTRACT

Amphotericin B (AmB) is one of the toxic drugs that with appropriate micelles structure for encapsulation can be effectively used in fungal infections and leishmaniasis treatments. The present work focuses on the design and development of micelles containing amphotericin B to decrease toxicity and improve antifungal activity. To this end, AmB was encapsulated in 1, 2-distearoyl-S-glycero-3-phosphorylcholine (DSPC) based micelles in the sensitive range of structural change with different ratios of DSPC and DSPE-PEG2000 (10:1, 9:2, 8:3; w/w) using the solvent evaporation method in methanol/chloroform medium. The effect of solvent composition and the combination of different ratios on the morphological and structural characteristics of unloaded and drug-loaded micelles were investigated by TEM and FESEM analyses. With a ratio of 9:2 w/w, spherical shape, and more uniform were successfully synthesized and considered as an optimal preferable microstructure for drug loading. Moreover, due to the slow release of the micelles system, the maximum drug release within 72 hours in the buffer environment is 86.2 %. The DLS analysis reported the mean particle size of drug-loaded Micelles as 55.1 nm and unloaded micelles as 51.6 nm. TEM-based particle size determination of the AmB-loaded sample revealed that the mean diameter of the micelles with optimum formulation was 27 ± 0.7 nm and for unloaded micelles 24 ± 0.6 nm. Furthermore, the Cytotoxicity of the AmB's micelles was tested using the MTT assay. In addition, *S. aureus, E. coli, and C. Albicans strains* were employed during the antimicrobial and antifungal tests.

How to cite this article
Nemati M. M., Tanidehvar M. M., Derakhshan E., Jafari Doudaran P., Mahdood B., Roostaie M., Assessing the cytotoxic functionality of Co-CeO2 nanoparticles towards colon cancer and mouse embryo fibroblast cells. Nanomed Res J, 2023; 8(1): 37-49. DOI: 10.22034/nmrj.2023.01.004

INTRODUCTION

Amphotericin B (AmB) as a polyethylene macrolide antibiotic is widely used to combat invasive systemic mycosis and leishmania[1, 2]. Its antifungal mechanism of action includes binding with the ergosterol on the fungal cell membrane while subsequent intracellular cations leakage leads to increased cell membrane permeability and cell death [3]. AmB has serious dose-dependent side effects including; nephrotoxicity, cardiotoxicity, hepatoxicity, hemolysis, leukopenia, thrombocytopenia, poor water solubility, and low bioavailability due to its aggregation pattern in solution which is originated from its amphiphilic structure [4, 5]. The injection of AmB as colloidal dispersion in sodium deoxycholate may cause adverse side effects because of quick release and aggregation while dilution in plasma. Several marketed formulations have been developed to improve patient tolerability and reduce the toxicity of AmB by decreasing its state and extent of aggregation, namely lipid or complexes, cholesteryl sulfate complexes, and liposomal formulations [6-9]. Moreover, several strategies are suggested for preparing AmB-loaded carrier systems such as

* Corresponding Author Email: *attar.h@srbiau.ac.ir*

nanoprecipitation [10], solvent diffusion method [11], Pickering emulsion [12], hydrotrope dilution [13], ionic gelation [14], and solvent evaporation method [15].

Polymeric micelles are submicron bilayer vesicles that are used in various medical fields and these nanoparticles serve as carriers of drugs and biologically active agents such as pharmaceuticals, cosmetics, and nutraceutical liposomes [16-20]. They are mostly composed of phospholipids as amphiphilic molecules with a hydrophilic head and hydrophobic tail groups [21, 22]. These newly-emerged nanostructured materials are the center of attention in various applications and nano therapy owing to their excellent and unique characteristics including biocompatibility, biodegradability, slow drug release, and nanosize [23-26]. Polymeric micelles are capable of improving the performance of bioactive agents by preventing their undesired intermolecular interactions, as well as enhancing their bioavailability, solubility, and stability (*in vitro* and *in vivo)* [27]. As another advantage, the utilization of micelles in cell-specific targeting paves the way for obtaining appropriate drug concentrations for optimum therapeutic efficacy in the target site with minimum adverse health impacts on normal cells and tissues [28-30].

Self-arrangement of hydrated phospholipid molecules into bilayer nanostructures has not to be considered a spontaneous process. In other words, from an equilibrium thermodynamics point of view, a certain quantity of energy should be supplied to the aqueous system in the form of homogenization, heating, sonication, etc. [31]. The most common micelles preparation techniques are sonication [32], extrusion [33], microfluidization [34], and heating [35]. The sonication-assisted solvent evaporation technique is a cost-effective and straightforward method that has attracted significant attention due to its potential to provide a smaller mean particle size and better dispersity [36, 37]. Among phospholipids, Distearoylphosphatidylcholine (DSPC), is often used as a major component of the formation of micelles and liposomes for many practical applications, On the other hand, PEGylated lipids such as 1, 2-distearoyl-Sn-glycero-3-phosphoethanolamine-N-[methoxy (polyethylene glycol)-2000] (DSPE-PEG2000), show latent properties due to the presence of PEG in their structure. It usually prolongs the circulation time in the blood by preventing the interaction between blood components and colloidal nanoparticles. it also prevents adsorption by macrophages of the reticuloendothelial system (RES) and this improves the biopharmaceutical properties of nanoparticles [38-45].

Dos Santos et al [46] showed that adding only 0.5 mol% of PEG2000-DSPE to DSPC liposomes significantly increased the plasma circulation and that 2 mol% PEG2000-DSPE in liposomes completely prevent the aggregation. Some studies have used cholesterol to Increase membrane flexibility and stability, but since cholesterol is required for macrophage internalization and parasite survival, For the treatment of leishmaniasis, cholesterol-free drug carriers are better compounds as vehicles [47].

In recent years, some research has been done on the preparation of DSPC and DSPE-PEG liposomal structures by combining different percentages and investigating different physicochemical properties and environmental effects on the formation of these structures[39,48,49]. However, the development of nanocarriers still faces challenges. The synthesis of PEG-DSPE liposomes is somewhat expensive[50], along with many benefits such as biocompatibility and FDA approval. Minor changes in the percentage composition of DSPC and DSPE-PEG2000 concentrations have significant effects on the shape of the micelles, the aggregation, and the drug loading percentage[51]. Therefore, it is necessary to achieve the accurate design and optimal percentage combination for the production of micelles to load amphotericin B using two specific lipids by creating different concentrations in the range of structural change 2 to 10 mol% of DSPE-PEG2000[51].

To our knowledge, this is the first study of its kind to use for the production of DSPC based micelles to achieve an optimal percentage composition with the spherical structure, nano-sized, high drug loading percentage with slow drug release for encapsulation of amphotericin B. The stability of micelles, particle size distribution, and their microstructural properties, as well as the cytotoxicity, antimicrobial and antifungal activity of AmB, loaded nanoparticles, were investigated.

MATERIALS AND METHODS

Materials

1, 2-Distearoyl-sn-glycero-3-phosphocholine (DSPC), 1, 2-distearoyl-sn-glycero-3-phosphoethanolamine-N-[methoxy(polyethylen eglycol)-2000] (DSPE-PEG2000) were procured from Avanti polar (Alabaster, AL, USA). Methanol

and chloroform (HPLC grade) were supplied by Sigma-Aldrich (St. Louis, MO, USA). AmB was obtained from Merck (Darmstadt, Germany). The K_2HPO_4 and KH_2PO_4 (sodium phosphate buffer reagent) were purchased from Merck (Germany). The Pasteur Institute Cell Bank prepared the Vero cell line. Antimicrobial tests were performed using bacterial strains (S. aureus (PTCC1112), E. coli (PTCC1399), C. Albicans (PTCC5027)) obtained from the Bank of Iranian Research Organization for Science and Technology (IROST) All the other reagents without further purification were used in analytical grade.

Micelles preparation and AmB encapsulation

Micelles were prepared using ultrasonication followed by the solvent evaporation method [48] with slight modifications. Three different formulations of DSPC and DSPE-PEG were provided as 10:1, 9:2, 8:3 ratios (DSPC: DSPE-PEG2000; w/w) and dissolved in the methanol -chloroform mixture (1:3 v/v). The mixtures were ultrafiltered to remove solid insoluble components and eliminate pyrogens. The filtered solutions were transferred to a round-bottom flask and the solvents were removed by using a rotary evaporator (Heidolph Instruments, Germany) at 65 °C under the vacuum, leaving what remained in the flask was a thin layer of lipid components. The ratio of 9:2 w/w that had the best result among the three compounds was chosen for the drug loading. Then, sodium phosphate buffer (pH 7.4), as a hydration medium, was added to the flask containing the dried lipids simultaneously with 1mg AmB. A magnetic stirrer was utilized for 5 minutes to agitate the mixture and disperse the dried lipids into the hydration fluid. At this point, micrometric structures are formed in the form of multilamellar vesicles (MLV). To reduce the size of the micelles to nano micelles, a sonication step was performed using a probe sonicator. The MLV flask was sonicated with an ultrasonic homogenizer (UHP-400, Topsonics) for 3 minutes under certain amplitude and time conditions, and small, unilamellar vesicles (SUV)-type micelles were consequently formed.

Characterization of AmB loaded micelles
Dynamic light scattering (DLS) analysis

DLS studies of the free and drug-loaded micelles using a Zeta A- check (Particle Metrix, Germany) equipped with a 532 nm laser at a back-scattering angle of 173° at 24 ± 1 °C. The polydispersity index (PDI) and the intensity average of the hydrodynamic diameter were measured using the cumulative analysis of the photon correlation function.

Encapsulation Efficiency (EE) and AmB Release Study

Evaluation of AmB release kinetics from polymeric micelles was performed using the dialysis method in vitro and encapsulated AmB was determined as follows. The encapsulation efficiency (EE) was obtained by determining the unencapsulated amount of amphotericin. For this purpose, the sonicated micelles containing 1 mg drug were transferred into the dialysis bag (Cut off 12-14 kDa) and the contents are incubated for one hour in 100 ml PBS buffer until the unencapsulated free drug was removed. During the next step, the absorption of unencapsulated AmB was calculated at a maximum wavelength of 408 nm by a spectrophotometer. Finally, using the standard diagram of AmB and equation 1, encapsulation efficiency was calculated.

For AmB release kinetics from polymeric micelles, Each micelle solution was dialyzed against excess PBS buffer (20). The release rate of AmB from micelles was determined the by membrane diffusion technique. The micellar suspension containing 1 mg AmB was poured into the dialysis bag (cut kDa 12-14). Then, a 100 ml container containing saline phosphate buffer (PH 7.4) was used to place the dialysis bag. After placing the dialysis bag in the container, Sampling (100 µl) was performed from the buffer medium around the dialysis bag at 1,3,6,12,18,24,48 and 72 h. After each sampling, an equal volume of phosphate buffer has been added.

Finally, the AmB calibration equation in the PBS (Equation 2) was used to calculate drug release concentrations at different times within 72 hours and the acquired data were plotted.

Morphology observations

Transmission electron microscopy (PHILIPS CM30 NETHERLANDS V = 200KV) was used to determine the surface morphology of micelles. Before the fixation on the mesh grids, the micellar suspension was diluted with deionized water and stained. After removing the residual solution, the samples were studied at 200 kV.

The morphological characteristics of the

$$EE\ (\%) = \frac{encapsulated\ AmB\ concentration}{Total\ amount\ of\ AmB\ concentration} \times 100 \quad \text{Equation 1}$$

$$DL\ (\%) = \frac{(Total\ amount\ of\ AmB - amount\ of\ uncapsulated\ AmB)}{Total\ amount\ of\ AmB} \quad \text{Equation 2}$$

$$\%\text{Cell viability results} = \frac{\text{Toxic by treatment of Adsorption Optical Cells} - \text{Optical Absorption Blank}}{\text{Optical Control of Adsorption} - \text{Optical Absorption Blank}} \times 100 \quad \text{Equation 3}$$

synthesized micelles were studied by field-emission scanning electron microscopy (FESEM) (TESCAN MIRA3, Czech Republic). To prepare SEM samples, a droplet of each one of the synthesized micelles solutions was cast on the mica sheet and then dried at room temperature and mounted on a double-faced adhesive tape afterward. After gold-plating by sputtering, the samples were observed at the accelerating voltage of 20 kV.

Cytotoxicity assay of the micelles

Cell culture: Vero cell lines that are resistant and sensitive were purchased from Pasteur Institute Cell Bank and cultured in the 90% DMEM and 10% fetal bovine serum medium containing 100 U/mL penicillin and 100 µg/mL streptomycin at37 °C and 5% carbon dioxide concentration with the humidity of about 80%. The cells were grown until 80% confluence. Confluent cells were passaged and plated at 1:2 or 1:3 dilutions using 0.25% trypsin and 1mM Ethylenediaminetetraacetic acid (EDTA) (Invitrogen LT, Merelbeke, Belgium) every 3–4 days. The cells were frozen in 20% serum and 10% DMSO (Merck, Darmstadt, Germany) in liquid nitrogen.

MTT assay: Cell suspensions were seeded into the 96-well-plate and incubated for 24 h (5- 6×103 per well). The cells were rested for at least 24 hours, which is equivalent to one cell cycle duration of selected cells, to achieve exponential growth. The 100 µL medium was added to each well After removing the previous medium, The cells were incubated with 10 µL of 5 mg/ml 3-(4, 5- dimethylthiazol-2-yl)-2, 5-diphenyltetrazolium bromide (MTT), which was dissolved in 90 µL of the medium after each treatment for 4 h. Tetrazolium yellow salt was cleaved by living cells into an insoluble precipitate (formazan). The decrease in the percentage of living cells is correlated with the amount of formazan precipitate crystals. After the supernatant was discarded, formazan precipitate was kept and DMSO (100 µL) was added into the wells. The absorbance of the specimen was measured at 570 nm with BioTek [49] microplate reader. The cell viability percentage is calculated using Equation 3 after contact with the samples at different concentrations. Compared to the control group, cell viability results were shown as a percentage. To quantify the sensitivity of selected cell types, the half-maximal inhibitory concentration (IC_{50}), which is the required concentration of AmB for a 50% inhibition of cell growth was measured. At least three independent repetitions were carried out for all of the experiments. Data were presented as mean ± SD (standard deviation). To determine the inhibitory concentration (IC50), GraphPad Prism 8 graphic fitting method was used to plot the values of the dose-response curve[49].

In vitro antifungal activity

Antimicrobial test: Antimicrobial tests were performed using bacterial strains of *S. aureus* (PTCC1112), *E. coli* (PTCC1399), and *C. Albicans*(PTCC5027)) from the Iranian Research Organization for Science and Technology (IROST). One gram-negative and two gram-positive strains were selected accordingly. In all assays, specific antibiotic standards were used to ensure the uniformity of the conditions of all tests and a comparative study based on the standards recommended by the National Committee for Clinical Laboratory Standards (NCCLS, 1997). Specific standard antibiotics were used for the gram-negative sample of streptomycin, the gram-positive sample of vancomycin, and the fungal sample of the chloramphenicol standard.

Cultivation and preparation of samples

All strains were stored at -70 °C before cultivation in a medium containing 11% (v / v) dimethyl sulfoxide. The bacterial and fungal strains were grown on Müller-Hinton agar and Saburod

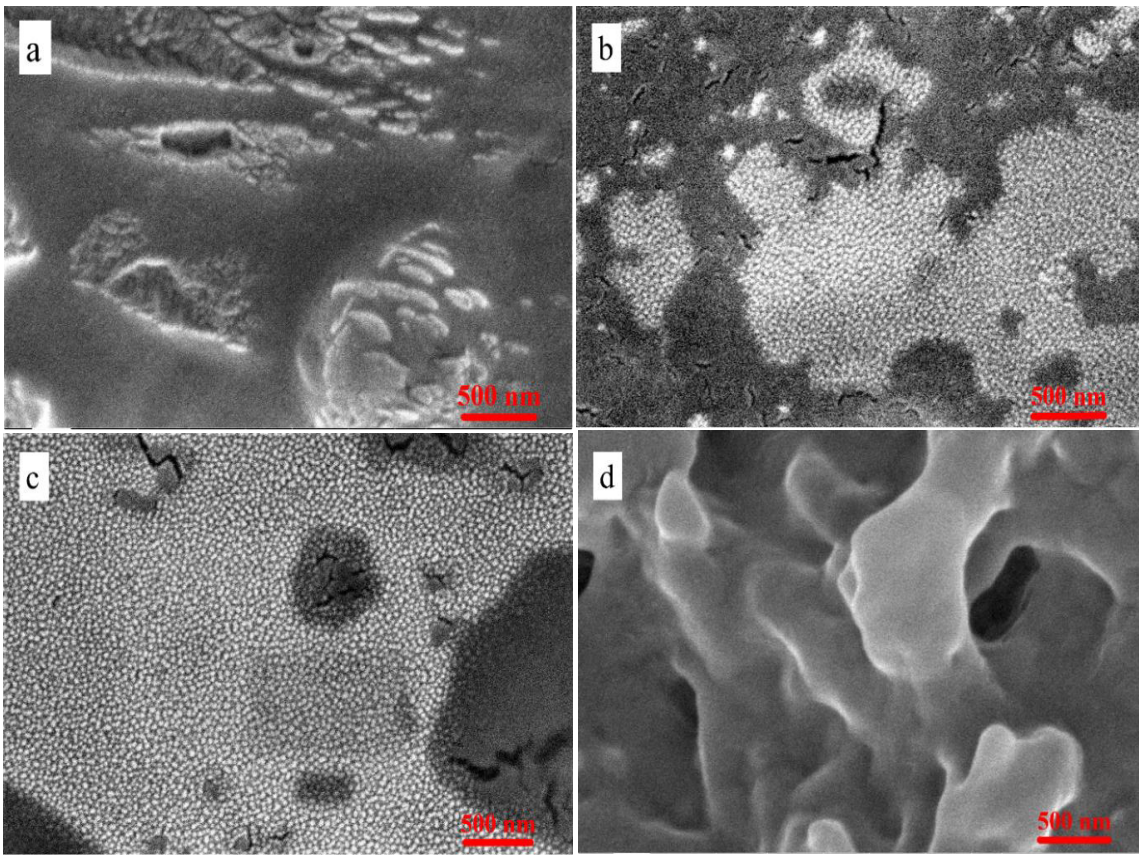

Fig. 1. FE-SEM images of surfaces of DSPC: DSPE-PEG2000 micelles with ratios of a) 8:3, b) 9:2 unloaded, c)drug-loaded 9:2, d) 10:1

dextrose agar plates (Merck, Germany) at 28 °C and 37 °C for fungal and bacterial samples, respectively. Single colonies of bacterial samples were cultured linearly in culture medium plates and incubated for 24 h. After two consecutive inoculations, the samples were rejuvenated and prepared for the next steps.

The inoculum consists of a suspension of microorganisms in the culture medium with about 106 colony-forming units (CFUs). To prepare the cell suspension, pure bacterial colonies were added to the 10 ml of Müller-Hinton broth medium, and after 30 seconds vortex for 4 h incubated. The sample concentration in this period was equal to turbidity as half of McFarland's visually or 0.5-0.6 in light absorption of 600 nm and pure colonies were used to prepare the inoculum (approximately 1.5 × 106 CFU / ml).

Assay of antimicrobial effect by disk diffusion method

For this purpose, 100 µl of inoculum of bacterial and fungal strains were cultured by grass sterilization on plates of sterile Müller Hinton agar media. Antibiogram paper disks (6 mm) were saturated with 30 µl of the synthesized nanoparticle colloids. The resulting discs were tested on strain grass plates and 37 ° C was used to keep the plates in the incubator. The diameter of the growth auras around the discs was determined by a caliber after 18 h. The standard antibiotic discs vancomycin, petomycin ester, and chloramphenicol were also used as positive controls.

RESULTS AND DISCUSSION

Morphology

The TEM (Fig. 2) and FE-SEM (Fig. 1(micrographs of micelles with different formulations are presented. As can be seen, the DSPC based micelles with a DSPC: DSPE-PEG ratio of 10:1 are synthesized in a disk shape (Fig. 2.d) which is in line with the results presented by Markus Johnsson et al. For low concentrations of DSPE-PEG[51]. Micelles with a ratio of DSPC: DSPE-PEG 9: 2 are successfully synthesized in a spherical shape and with uniform dispersion compared to the other two formulations. Belsito et al. set the onset of micelle

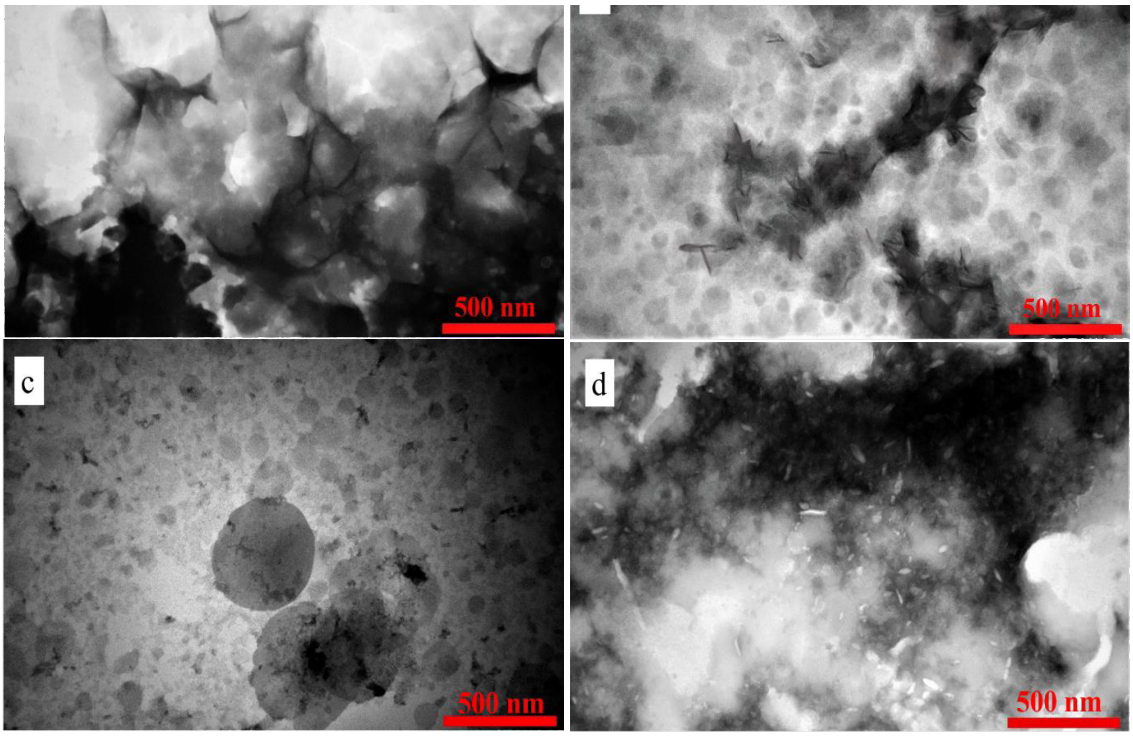

Fig. 2. TEM images of surfaces of DSPC: DSPE-PEG2000 micelles with ratios of a) 8:3, b) 9:2 unloaded, c)drug-loaded 9:2, d) 10:1

formation in the DSPC: DSPE-PEG formulation to 5 mol% which is consistent with the percentage composition of this study [52]. The structural evolution of DSPC: DSPC- PEG micelles change from disc-like micelles to spherical by increasing the PEG-lipid content [51]. From the TEM picture (Fig. 2. a), it can be seen that in DSPC: DSPE-PEG 8:3 formulation the size of the micelles decreases with increasing PEG-lipid concentration, and aggregation occurs(Fig. 1. a). Therefore, the authors have chosen DSPC: DSPE-PEG ratio of 9:2 formulation, and it was considered as the optimized formulation from the microstructural and morphological point of view.

According to FESEM and TEM pictures, the drug-loaded and unloaded DSPC-PEG spherical micelles with DSPC: DSPE-PEG ratio of 9:2 are formed with a homogeneous dispersion. Furthermore, the mean diameter of the synthesized micelles can be determined by using microscopy images. Accordingly, the mean diameter of the micelles with optimum formulation was 24 ± 0.6 nm. The results show that the AmB-loaded DSPC-PEG spherical micelles are not morphologically different from unloaded ones. It suggests that the encapsulation of AmB into the micelles had no significant influence on the morphology of the drug-loaded micelles. Furthermore, TEM-based particle size determination of the AmB-loaded sample revealed that the mean diameter of the micelles with optimum formulation was 26 ± 0.6 nm. Thus, it can be concluded that the encapsulation of AmB into the DSPC-PEG micelles barely affects their morphology and slightly increases their size.

Mean particle size and size distribution of micelles

Particle size and polydispersity index (PDI) are among the most influential parameters on stability, distribution, and compound release [31, 53]. According to Fig. 3, the DLS measurements demonstrate that the drug-loaded and unloaded DSPC-PEG micelles fell within the nanosize range which is desirable for most applications. The particle size and PDI results are illustrated in Table 1. It could be concluded that the size of the DSPC: DSPC-PEG spherical micelles is slightly increased after the incorporation of AmB molecules which is in agreement with the literatures [54, 55]. To determine whether particles are monodisperse or polydisperse, PDI is a good measure to show dispersion. PDI values for both AmB-loaded and unloaded micelles were lower than 0.2 which indicates that the homogeneous suspensions with narrow dispersity were obtained [56, 57].

Table 1. Mean diameter and PDI of micelles.

	Mean diameter (nm)		PDI
	TEM	DLS	
Unloaded sample	24 ± 0.6	51.6	0.19
Drug-loaded sample	27 ± 0.7	55.1	0.06

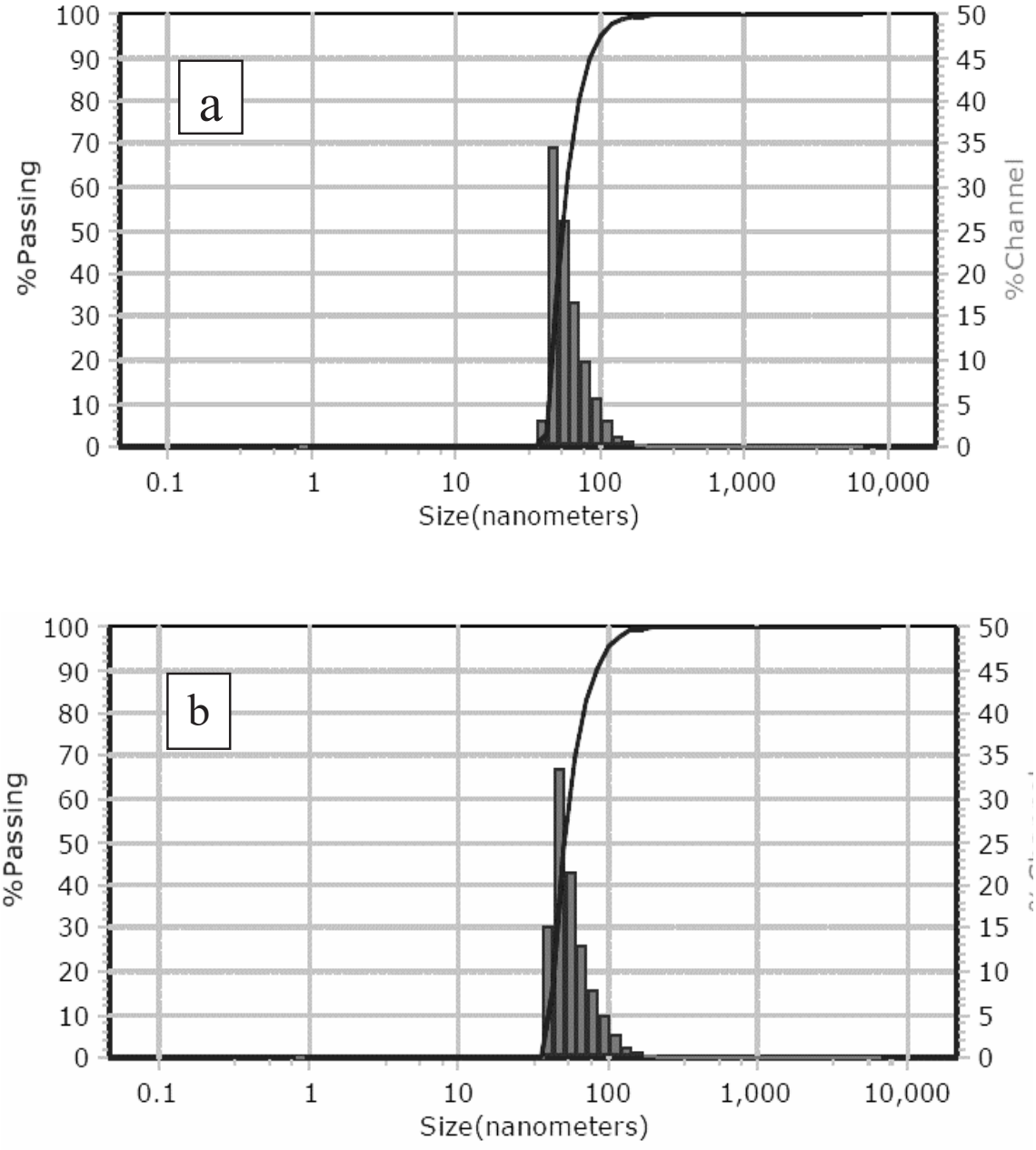

Fig. 2. TEM images of surfaces of DSPC: DSPE-PEG2000 micelles with ratios of a) 8:3, b) 9:2 unloaded, c)drug-loaded 9:2, d) 10:1

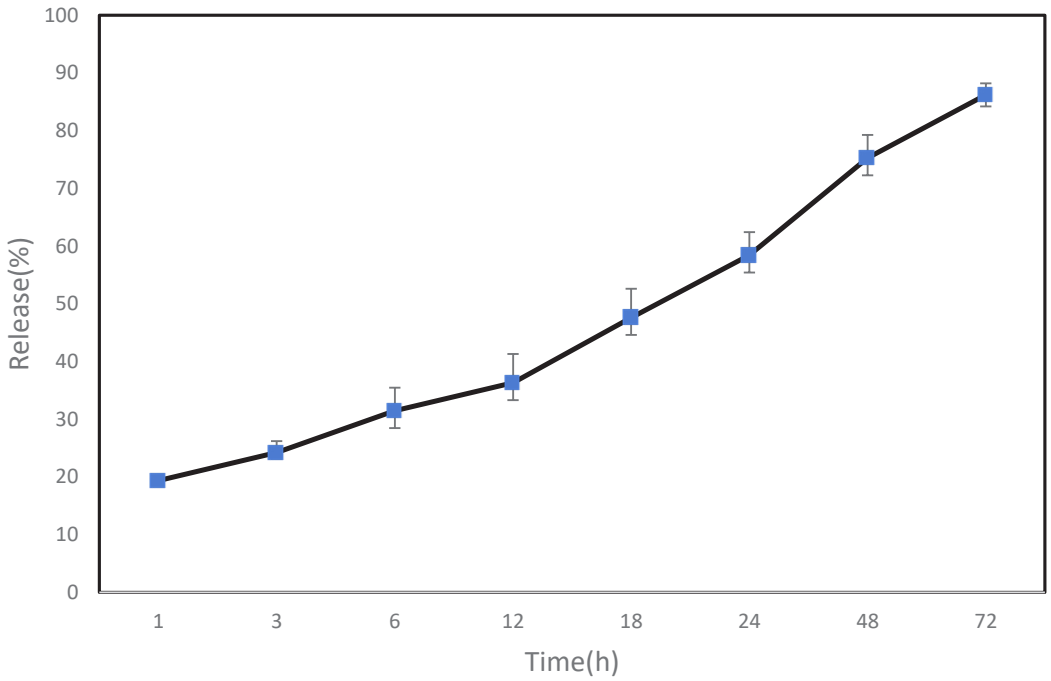

Fig 4. AmB drug release chart from micelles during 72 h (mean ± SD, n = 3)

On the other hand, as indicated in Table 1, the experimental values of the hydrodynamic diameters derived from the DLS measurement for both AmB-loaded and unloaded samples are significantly higher than that of the mean diameters measured from the TEM micrographs. It could be associated with the fact that the PEG is a soluble component in DLS medium giving rise to a swollen structure with high water content and as expected, greater particle size [49, 58].

In vitro release of micelles

AmB release from micelles was assessed at room temperature (25°C) using a dialysis bag soaked in PBS release medium to guarantee sink conditions. UV-vis spectroscopy was used to monitor the concentration of AmB released into the medium at 408 nm. The release profiles were illustrated in Fig. 4. The drug encapsulation efficiency is 80.63% while confirming the slow release of the micelle system. During the 72 hours, AmB is released slowly to achieve a cumulative release of nearly 86.2 % of the loaded drug. After 72 hours, the release rate consistently reached its maximum release rate. Compared to the release of free amphotericin B reported by other authors about 98.7% in the first 24 hours, in this study, there was no burst release phenomenon from the micelles loaded with AmB[59]. In formulations based on nanoparticles, sustained release is the most desirable form of release, and release can follow a linear graph as a function of the square root of time, as in our research. The long-term release is critical in chronic disease where repeated dosing is not preferred [60].

Cytotoxicity assay of the micelles

Cytotoxicity of AmB-loaded micelles was evaluated using Vero cells by MTT assay. Different concentrations of free AmB and AmB loaded micelles, and unloaded micelles were evaluated for cell viability (%) accordingly. While the cytotoxicity of AmB was significantly reduced by the use of micelles, AmB reduced cell viability in a manner commensurate with dose changes. The cell viabilities of free AmB were much less than those AmB loaded micelles and unloaded micelles. It could be observed that the MTT results had no significant differences after 24 or 48 h. Both these results proved that AmB loaded micelles and unloaded micelles were less cytotoxic than free AmB.

A comparative study of the IC_{50} content of AmB micelles on the Vero cell line was presented in Table 2. The IC_{50} levels were almost slightly different. According to Fig. 5, which is in terms of viability for concentrations below 50 µg/ml, the first significant

Table 2. Comparative study of IC_{50} amphotericin B micelles on Vero cell line

	NM	Amb	NM-AmB
IC_{50}(µg/ml)	109.3±21.71	51.95±11.92	56.09±7.474

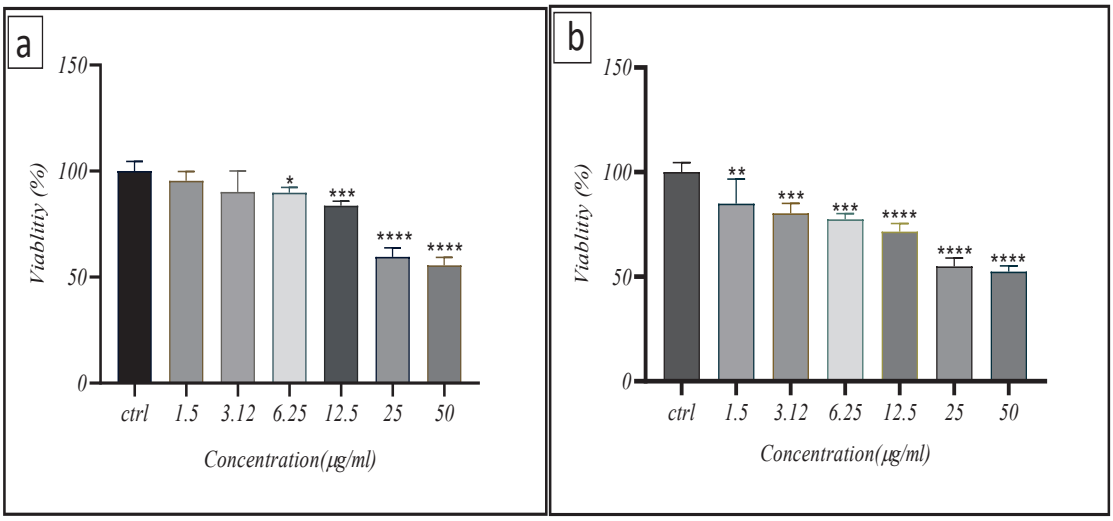

Fig. 5. The effect of different concentrations of amphotericin B on the viability of Vero cells. a) AmB loaded Micelles (NM-AmB). b) Free AmB.

difference with control occurs at 6.25 µg/ml with 89.82% viability for AmB loaded micelles, whereas, for the free AmB, it starts only at 1.5 µg/ml with almost similar viability. cells. This means that the effect of the drug on cell viability in the micelles state loaded with AmB is much greater than that of the free drug, and the slope of cell destruction for the free drug is very steep.

Antifungal and antimicrobial assay

A wide range of research works have been performed on the antifungal activity of AmB-encapsulated nanocarriers and it is concluded that the effectiveness of AmB is profoundly increased as an antifungal drug [61]. The compounds used in the preparation of drug nanoparticles are very important and in addition to creating nano-based formulations, can be effective in intensifying drug activity. In the study of Yien et al., the fungicidal effect of Trimethyl chitosan alone on Candida albicans at the concentration of 0.2 mg / mL had been reported[62]. Also, in another study conducted by Palmeira et al., it was suggested that tripolyphosphate alone has fungicidal properties and its use as a crosslinking agent in the nanoformulation composition has an antifungal effect similar to the amphotericin B [63]. Therefore, the compounds used with the determined formulation have a significant role in increasing the antifungal effects on the drug nanoparticles in this study and can be used as a carrier for fungal antibiotics in other studies.

In this work, the effect of different dilutions of AmB unloaded and loaded into DSPC-PEG micelles on bacterial strains of *S. aureus*, *E. coli* was investigated using *in vitro* method. In microbial tests related to both *S. aureus* and *E. coli* strains, Studies have shown that drug micelles have antimicrobial effects on the studied microbial strains and inhibit their growth. The inhibitory effect of drug-containing micelles on gram-negative bacteria was less than that of gram-positive bacteria. Comparison of IZs related to free drug and micelles form with control antibiotics showed that its antimicrobial effect was less than that of antibiotics used.

On the other hand, the antifungal assay was performed on *C. Albicans*. The results of the

Table 3. Antimicrobial and antifungal effect of compounds in three concentrations. IZ: Inhibition Zone (mm).

Concentration (µg/ml)	*S. aureus* (PTCC1112)		*E. coli* (PTCC1399)		*C. albicanse* (PTCC5027)	
	IZ (mm)		IZ (mm)		IZ (mm)	
	24h	48h	24h	48h	24h	48h
Amb 100(µg/ml)	16±1	16±1	14±1	14±1	20±2	20±1
Amb 50(µg/ml)	14±1	14±1	10±1	10±1	19±1	19±1
Amb 25 (µg/ml)	10±1	10±0.5	8±0.5	8±0.5	16±1	16±1
NM 100(µg/ml)	7±0.5	7±0.5	-	-	8±0.5	8±0.5
NM 50(µg/ml)	-	-	-	-	-	-
NM 25 (µg/ml)	-	-	-	-	-	-
NM-Amb 100(µg/ml)	15±0.5	16±1	12±1	12±1	21±1	22±1
NM-Amb 50(µg/ml)	11±1	12±1	8±0.5	8±0.5	20±1	21±1
NM-Amb 25 (µg/ml)	9±0.5	10±0.5	-	-	17±0.5	17±1
Streptomycin	-	-	18±1	18±1	-	-
Vancomycin	18±1	18±1	-	-	-	-
Chloramphenicol	-	-	-	-	12±2	12±2

antifungal assay revealed that the AmB-loaded DSPC-PEG micelles remarkably reduce the growth of *C. Albicans* compared to the control sample.

AmB loaded micelles showed the same high antifungal activity as free AmB in biological studies, while unloaded micelles had no significant effect. In the case of drug-loaded micelles, After 24 and 48 hours, the inhibition zone grows in a semi-halo, which may be explained by the process of drug release from the micelles, while the free drug is immediately available. In addition, considering that the mechanism for AmB activity seems to be related to the formation of multimeric drug associations, it could be possible that the drug released from the micelles is partially in conformation with the target interaction. This confirms the fact that the growth of *C. Albicans* biofilms is further inhibited at lower doses of AmB-loaded micelles. It may indicate that these micelles presented a superior penetration ability to pass through the extra-polymeric matrix and interact with the membrane of *C. Albicans*. According to the results presented in Table 3, the greatest difference in fungal growth inhibition in drug nanoparticles and the traditional form was observed at a concentration of 50 µg/ml. For a concentration of 100 µg/ml of traditional drug, IZ is equal to 20 in 48 hours, while for drug-loaded micelles the same IZ occurred in 24 hours and at

a concentration of 50 µg/ml. There is a significant difference between the results in inhibiting and suppressing the fungal growth at lower doses. These results are consistent with observations made by other researchers on the nano-delivery of AmB [64, 65].

It seems that the desired result of cytotoxicity of micelles containing AmB and at the same time strong antifungal and antimicrobial effects is related to the presence of molecules of the drug in the monomers form in micelles, which shows an interesting practical application. The monomeric form of the drug is toxic only to fungal cells, while self-aggregated AmB is reportedly toxic to both fungal and mammalian cells [66].

The presence of a detectable susceptibility pattern for *C. Albicans* and the *in vitro* antifungal effect of synthesized nanoparticles in this study suggest that the present formulation has increased the potency of the drug at lower doses. Finally, this study revealed that the prepared nano-drug can be used as a promising formulation in the preparation of AmB for the treatment of fungal patients, due to the precise balance between toxicity and antifungal efficacy.

CONCLUSIONS

In this study, DSPC based polymeric micelles were prepared using the solvent evaporation method in three different concentrations of DSPC and DSPE-PEG2000 (10:1, 9:2, 8:3 ratios). The effect of solvent composition and the combination of different ratios on the morphological and structural characteristics of unloaded and AmB loaded micelles were investigated by TEM and FESEM analyses. The 9:2 ratio of DSPC: DSPE-PEG was determined as the optimum concentration based on the homogeneous morphology of the synthesized micelles. AmB was loaded into the micelles with the optimum formulation and the TEM, DLS, and UV-vis spectrophotometry analyses were carried on. These results confirmed that the DSPC based micelles were successfully synthesized with uniform dispersion and a mean particle size of 26 ± 0.6 nm. The encapsulation of AmB into the micelles had no significant influence on the morphology of the drug-loaded micelles. To evaluate the performance of prepared micelles, an MTT assay was used for micellar cytotoxicity. antimicrobial tests on bacterial strains of *S. aureus, E. coli,* and antifungal tests on *C. Albicans* were investigated *in vitro*. Finally, it can be concluded that the prepared micelles can be used as a suitable structure for AmB delivery with the desired fungal and microbial treatment impacts.

CONFLICT OF INTEREST

The authors declare no conflict of interest.

REFERENCES

1. Sombra, F.M., et al., Development of amphotericin B-loaded propionate Sterculia striata polysaccharide nanocarrier. International journal of biological macromolecules, 2020. 146: p. 1133-1141. https://doi.org/10.1016/j.ijbiomac.2019.10.053
2. Biswas, S., et al., Polymeric micelles for the delivery of poorly soluble drugs. Drug Delivery Strategies for Poorly Water-Soluble Drugs, 2013: p. 411-476. https://doi.org/10.1002/9781118444726.ch14
3. Nemati Shizari, L., et al., A New Amphotericin B-loaded Trimethyl Chitosan Nanoparticles as a Drug Delivery System and Antifungal Activity on Candida albicans Biofilm. Archives of Razi Institute, 2020.
4. Song, Z., et al., Linolenic acid-modified methoxy poly (ethylene glycol)-oligochitosan conjugate micelles for encapsulation of amphotericin B. Carbohydrate polymers, 2019. 205: p. 571-580. https://doi.org/10.1016/j.carbpol.2018.10.086
5. Diezi, T.A., et al., Pharmacokinetics and nephrotoxicity of amphotericin B-incorporated poly (ethylene glycol)-block-poly (N-hexyl stearate l-aspartamide) micelles. Journal of pharmaceutical sciences, 2011. 100(6): p. 2064-2070. https://doi.org/10.1002/jps.22445
6. Gaydhane, M., et al., Gelatin nanofiber assisted zero order release of Amphotericin-B: A study with realistic drug loading for oral formulation. Materials Today Communications, 2020. 24: p. 100953. https://doi.org/10.1016/j.mtcomm.2020.100953
7. de Paula, R.C.M., et al., Developing effective amphotericin B delivery systems for fungal infections, in Applications of Nanobiotechnology for Neglected Tropical Diseases. 2021, Elsevier. p. 119-139. https://doi.org/10.1016/B978-0-12-821100-7.00002-9
8. Lanza, J.S., et al., Recent advances in amphotericin B delivery strategies for the treatment of leishmaniases. Expert opinion on drug delivery, 2019. 16(10): p. 1063-1079. https://doi.org/10.1080/17425247.2019.1659243
9. Torrado, J., et al., Amphotericin B formulations and drug targeting. Journal of pharmaceutical sciences, 2008. 97(7): p. 2405-2425. https://doi.org/10.1002/jps.21179
10. Palma, E., et al., Antileishmanial activity of amphotericin B-loaded-PLGA nanoparticles: an overview. Materials, 2018. 11(7): p. 1167. https://doi.org/10.3390/ma11071167
11. Jansook, P., Z. Fülöp, and G.C. Ritthidej, Amphotericin B loaded solid lipid nanoparticles (SLNs) and nanostructured lipid carrier (NLCs): physicochemical and solid-solution state characterizations. Drug development and industrial pharmacy, 2019. 45(4): p. 560-567. https://doi.org/10.1080/03639045.2019.1569023
12. Richter, A., et al., Pickering emulsion stabilized by cashew gum-poly-l-lactide copolymer nanoparticles: Synthesis,

characterization and amphotericin B encapsulation. Colloids and Surfaces B: Biointerfaces, 2018. 164: p. 201-209. https://doi.org/10.1016/j.colsurfb.2018.01.023
13. Jain, S., et al., Lyotropic liquid crystalline nanoparticles of amphotericin B: implication of phytantriol and glyceryl monooleate on bioavailability enhancement. AAPS PharmSciTech, 2018. 19(4): p. 1699-1711. https://doi.org/10.1208/s12249-018-0986-3
14. Senna, J.P., et al., Dual alginate-lipid nanocarriers as oral delivery systems for amphotericin B. Colloids and Surfaces B: Biointerfaces, 2018. 166: p. 187-194. https://doi.org/10.1016/j.colsurfb.2018.03.015
15. Ludwig, D.B., et al., Antifungal activity of chitosan-coated poly (lactic-co-glycolic) acid nanoparticles containing amphotericin B. Mycopathologia, 2018. 183(4): p. 659-668. https://doi.org/10.1007/s11046-018-0253-x
16. Panahi, Y., et al., Recent advances on liposomal nanoparticles: synthesis, characterization and biomedical applications. Artificial cells, nanomedicine, and biotechnology, 2017. 45(4): p. 788-799. https://doi.org/10.1080/21691401.2017.1282496
17. Rehman, A., et al., Carotenoid-loaded nanocarriers: A comprehensive review. Advances in colloid and interface science, 2020. 275: p. 102048. https://doi.org/10.1016/j.cis.2019.102048
18. Aguilar-Pérez, K., et al., Insight Into Nanoliposomes as Smart Nanocarriers for Greening the Twenty-First Century Biomedical Settings. Frontiers in Bioengineering and Biotechnology, 2020. 8: p. 1441. https://doi.org/10.3389/fbioe.2020.579536
19. Saadat, E., et al., Polymeric micelles based on hyaluronic acid and phospholipids: Design, characterization, and cytotoxicity. Journal of Applied Polymer Science, 2014. 131(20). https://doi.org/10.1002/app.40944
20. Wu, Y., F.B. Che, and J.H. Chen, Synthesis and characterization of an amphiphilic pluronic-poly (D, L-lactide-co-glycolide) copolymer and their nanoparticles as protein delivery systems. Journal of applied polymer science, 2008. 110(2): p. 1118-1128. https://doi.org/10.1002/app.28723
21. Hamadou, A.H., et al., Formulation of vitamin C encapsulation in marine phospholipids nanoliposomes: Characterization and stability evaluation during long term storage. LWT, 2020. 127: p. 109439. https://doi.org/10.1016/j.lwt.2020.109439
22. Vandermeulen, G., et al., Encapsulation of amphotericin B in poly (ethylene glycol)-block-poly (ε-caprolactone-co-trimethylenecarbonate) polymeric micelles. International journal of pharmaceutics, 2006. 309(1-2): p. 234-240. https://doi.org/10.1016/j.ijpharm.2005.11.031
23. Demirci, M., et al., Encapsulation by nanoliposomes. Nanoencapsulation technologies for the food and nutraceutical industries, 2017: p. 74-113. https://doi.org/10.1016/B978-0-12-809436-5.00003-3
24. Hallaj-Nezhadi, S. and M. Hassan, Nanoliposome-based antibacterial drug delivery. Drug delivery, 2015. 22(5): p. 581-589. https://doi.org/10.3109/10717544.2013.863409
25. Maherani, B., et al., Liposomes: a review of manufacturing techniques and targeting strategies. Current Nanoscience, 2011. 7(3): p. 436-452. https://doi.org/10.2174/157341311795542453
26. Usman, F., et al., Pharmacologically safe nanomicelles of amphotericin B with lipids: nuclear magnetic resonance and molecular docking approach. Journal of pharmaceutical sciences, 2017. 106(12): p. 3574-3582. https://doi.org/10.1016/j.xphs.2017.08.013
27. Banshoya, K., et al., Development of an amphotericin B micellar formulation using cholesterol-conjugated styrene-maleic acid copolymer for enhancement of blood circulation and antifungal selectivity. International Journal of Pharmaceutics, 2020. 589: p. 119813. https://doi.org/10.1016/j.ijpharm.2020.119813
28. Mozafari, M., Nanoliposomes: preparation and analysis, in Liposomes. 2010, Springer. p. 29-50. https://doi.org/10.1007/978-1-60327-360-2_2
29. Su, C., et al., Analytical methods for investigating in vivo fate of nanoliposomes: A review. Journal of pharmaceutical analysis, 2018. 8(4): p. 219-225. https://doi.org/10.1016/j.jpha.2018.07.002
30. Mozafari, M.R., Nanocarrier technologies: frontiers of nanotherapy. 2006: Springer. https://doi.org/10.1007/978-1-4020-5041-1
31. Reza Mozafari, M., et al., Nanoliposomes and their applications in food nanotechnology. Journal of liposome research, 2008. 18(4): p. 309-327. https://doi.org/10.1080/08982100802465941
32. Khatib, N., et al., Co-encapsulation of lupulon and xanthohumol in lecithin-based nanoliposomes developed by sonication method. Journal of Food Processing and Preservation, 2019. 43(9): p. e14075. https://doi.org/10.1111/jfpp.14075
33. Hadian, Z., et al., Preparation and characterization of nanoliposomes containing docosahexaenoic and eicosapentaenoic acids by extrusion and probe sonication. Iranian Journal of Nutrition Sciences & Food Technology, 2013. 8(1): p. 219-230.
34. Gulzar, S. and S. Benjakul, Characteristics and storage stability of nanoliposomes loaded with shrimp oil as affected by ultrasonication and microfluidization. Food Chemistry, 2020. 310: p. 125916. https://doi.org/10.1016/j.foodchem.2019.125916
35. Zarrabi, A., et al., Nanoliposomes and tocosomes as multifunctional nanocarriers for the encapsulation of nutraceutical and dietary molecules. Molecules, 2020. 25(3): p. 638. https://doi.org/10.3390/molecules25030638
36. Arabi, M.H., et al., Preparation methods of nanoliposomes containing Zataria multiflora essential oil: A comparative study. Bioscience and Biotechnology Research. Community, 2017. 10(1): p. 151-60. https://doi.org/10.21786/bbrc/10.1/23
37. Amiri, S., et al., New formulation of vitamin C encapsulation by nanoliposomes: Production and evaluation of particle size, stability and control release. Food science and biotechnology, 2019. 28(2): p. 423-432. https://doi.org/10.1007/s10068-018-0493-z
38. Mobed, M. and T. Chang, Comparison of polymerically stabilized PEG-grafted liposomes and physically adsorbed carboxymethyl chitin and carboxymethyl/glycol chitin liposomes for biological applications. Biomaterials, 1998. 19(13): p. 1167-1177. https://doi.org/10.1016/S0142-9612(98)00004-0
39. Silvander, M., M. Johnsson, and K. Edwards, Effects of PEG-lipids on the permeability of phosphatidylcholine/cholesterol liposomes in buffer and human serum. Chemistry and physics of lipids, 1998. 97(1): p. 15-26.

https://doi.org/10.1016/S0009-3084(98)00088-7
40. Ishida, O., et al., Liposomes bearing polyethyleneglycol-coupled transferrin with intracellular targeting property to the solid tumors in vivo. Pharmaceutical research, 2001. 18(7): p. 1042-1048. https://doi.org/10.1023/A:1010960900254
41. Cosco, D., et al., Aqueous-core PEG-coated PLA nanocapsules for an efficient entrapment of water-soluble anticancer drugs and a smart therapeutic response. European Journal of Pharmaceutics and Biopharmaceutics, 2015. 89: p. 30-39. https://doi.org/10.1016/j.ejpb.2014.11.012
42. Celia, C., et al., Improved in vitro anti-tumoral activity, intracellular uptake and apoptotic induction of gemcitabine-loaded pegylated unilamellar liposomes. Journal of nanoscience and nanotechnology, 2008. 8(4): p. 2102-2113. https://doi.org/10.1166/jnn.2008.065
43. Pasut, G. and F.M. Veronese, State of the art in PEGylation: the great versatility achieved after forty years of research. Journal of controlled release, 2012. 161(2): p. 461-472. https://doi.org/10.1016/j.jconrel.2011.10.037
44. Shan, X., et al., Influence of polyethylene glycol molecular weight on the anticancer drug delivery of pH-sensitive polymeric micelle. Journal of Applied Polymer Science, 2019. 136(32): p. 47854. https://doi.org/10.1002/app.47854
45. Zhou, W., et al., Factors affecting the stability of drug-loaded polymeric micelles and strategies for improvement. Journal of Nanoparticle Research, 2016. 18(9): p. 1-18. https://doi.org/10.1007/s11051-016-3583-y
46. Dos Santos, N., et al., Influence of poly (ethylene glycol) grafting density and polymer length on liposomes: relating plasma circulation lifetimes to protein binding. Biochimica et Biophysica Acta (BBA)-Biomembranes, 2007. 1768(6): p. 1367-1377. https://doi.org/10.1016/j.bbamem.2006.12.013
47. Mishra, J., et al., Evaluation of toxicity & therapeutic efficacy of a new liposomal formulation of amphotericin B in a mouse model. The Indian journal of medical research, 2013. 137(4): p. 767.
48. Tsermentseli, S.K., et al., Comparative study of PEGylated and conventional liposomes as carriers for shikonin. Fluids, 2018. 3(2): p. 36. https://doi.org/10.3390/fluids3020036
49. Jusu, S., et al., Drug-encapsulated blend of PLGA-PEG microspheres: in vitro and in vivo study of the effects of localized/targeted drug delivery on the treatment of triple-negative breast cancer. Scientific Reports, 2020. 10(1): p. 1-23. https://doi.org/10.1038/s41598-020-71129-0
50. Faustino, C. and L. Pinheiro, Lipid systems for the delivery of amphotericin B in antifungal therapy. Pharmaceutics, 2020. 12(1): p. 29. https://doi.org/10.3390/pharmaceutics12010029
51. Johnsson, M. and K. Edwards, Liposomes, disks, and spherical micelles: aggregate structure in mixtures of gel phase phosphatidylcholines and poly (ethylene glycol)-phospholipids. Biophysical Journal, 2003. 85(6): p. 3839-3847. https://doi.org/10.1016/S0006-3495(03)74798-5
52. Belsito, S., R. Bartucci, and L. Sportelli, Lipid chain length effect on the phase behavior of PCs/PEG: 2000-PEs mixtures. A spin label electron spin resonance and spectrophotometric study. Biophysical chemistry, 2001. 93(1): p. 11-22. https://doi.org/10.1016/S0301-4622(01)00201-0
53. Isailović, B.D., et al., Resveratrol loaded liposomes produced by different techniques. Innovative food science & emerging technologies, 2013. 19: p. 181-189. https://doi.org/10.1016/j.ifset.2013.03.006
54. Budhian, A., S.J. Siegel, and K.I. Winey, Haloperidol-loaded PLGA nanoparticles: a systematic study of particle size and drug content. International journal of pharmaceutics, 2007. 336(2): p. 367-375. https://doi.org/10.1016/j.ijpharm.2006.11.061
55. Kufleitner, J., et al., Adsorption of obidoxime onto human serum albumin nanoparticles: drug loading, particle size, and drug release. Journal of microencapsulation, 2010. 27(6): p. 506-513. https://doi.org/10.3109/02652041003681406
56. Hasan, M., et al., Chitosan-coated liposomes encapsulating curcumin: Study of lipid-polysaccharide interactions and nanovesicle behavior. RSC advances, 2016. 6(51): p. 45290-45304. https://doi.org/10.1039/C6RA05574E
57. Das, S. and A. Chaudhury, Recent advances in lipid nanoparticle formulations with solid matrix for oral drug delivery. Aaps Pharmscitech, 2011. 12(1): p. 62-76. https://doi.org/10.1208/s12249-010-9563-0
58. Yaszemski, M.J., et al., Tissue engineering and novel delivery systems. 2003: CRC Press. https://doi.org/10.1201/9780203913338
59. Wang, Y., et al., Biodegradable functional polycarbonate micelles for controlled release of amphotericin B. Acta biomaterialia, 2016. 46: p. 211-220. https://doi.org/10.1016/j.actbio.2016.09.036
60. Subramaniam, B., Z.H. Siddik, and N.H. Nagoor, Optimization of nanostructured lipid carriers: Understanding the types, designs, and parameters in the process of formulations. Journal of nanoparticle research, 2020. 22(6): p. 1-29. https://doi.org/10.1007/s11051-020-04848-0
61. de Bastiani, F.W.M.d.S., et al., Nanocarriers provide sustained antifungal activity for amphotericin B and miltefosine in the topical treatment of murine vaginal candidiasis. Frontiers in microbiology, 2020. 10: p. 2976. https://doi.org/10.3389/fmicb.2019.02976
62. Yien, L., et al., Antifungal activity of chitosan nanoparticles and correlation with their physical properties. International Journal of Biomaterials, 2012. 2012. https://doi.org/10.1155/2012/632698
63. Palmeira-de-Oliveira, R., et al., Sodium Tripolyphosphate: An excipient with intrinsic in vitro anti-Candida activity. International journal of pharmaceutics, 2011. 421(1): p. 130-134. https://doi.org/10.1016/j.ijpharm.2011.09.030
64. Lotfali, E., et al., In Vitro Activity of Two Nanoparticles on Clinical Isolates of Candida parapsilosis, Showing Resistance Against Antifungal Agents in Children. Archives of Clinical Infectious Diseases, 2017. 12(4). https://doi.org/10.5812/archcid.13853
65. Zia, Q., et al., Biomimetically engineered Amphotericin B nano-aggregates circumvent toxicity constraints and treat systemic fungal infection in experimental animals. Scientific reports, 2017. 7(1): p. 1-19. https://doi.org/10.1038/s41598-017-11847-0
66. Zhou, L., et al., Preparation, characterization, and evaluation of amphotericin B-loaded MPEG-PCL-g-PEI micelles for local treatment of oral Candida albicans. International journal of nanomedicine, 2017. 12: p. 4269. https://doi.org/10.2147/IJN.S124264